MAGNETOHYDRODYNAMICS Vol. 51 (2015), No. 2, pp. 237–247

PATTERNED TURBULENCE AS A FEATURE OF TRANSITIONAL REGIMES OF MAGNETOHYDRODYNAMIC DUCT FLOWS

D. Krasnov[1], *O. Zikanov*[2], *T. Boeck*[1]

[1] *Institute of Thermodynamics and Fluid Mechanics, Ilmenau University of Technology, 98684 Ilmenau, Germany*
[2] *Department of Mechanical Engineering, University of Michigan – Dearborn, MI 48128-1491, USA*

We present results of a numerical analysis of transition to turbulence and laminarization processes in magnetohydrodynamic duct flows with a transverse magnetic field. The simulations continue our earlier work [1, 2], where flow regimes with localized turbulent spots near the side walls parallel to the imposed magnetic field have been discovered. The new results extend the analysis to the case of large Reynolds and Hartmann numbers and to ducts of various aspect ratios. The results show good agreement with experiments and confirm that the states with localized turbulent spots are a robust feature of transitional magnetohydrodynamic duct flows.

Introduction. Flows of electrically conducting fluids in tubes (i.e. pipes and ducts) with an imposed transverse magnetic field and electrically insulating walls can be considered as archetypal for liquid metal magnetohydrodynamics (MHD). They combine, in a simple and well-defined setting, the key phenomena: flow transformation by the magnetic field and the effects of solid walls and mean shear. These flows are also of historical interest. They were the subject of the experimental work of Hartmann and Lazarus [3], which had led to the first theoretical result of the liquid metal MHD – the theory of the Hartmann boundary layer [4].

In this paper, we consider transition to turbulence and laminarization in MHD tube flows. The discussion is conducted in terms of the non-dimensional Hartmann and Reynolds numbers

$$\mathrm{Ha} \equiv aB\sqrt{\frac{\sigma}{\rho\nu}}, \;\; \mathrm{Re} \equiv \frac{aU}{\nu}, \tag{1}$$

where B is the induction of the imposed uniform magnetic field $\mathbf{B}$, a is the half-width of the duct, U is the mean velocity, and σ, ρ and ν are, respectively, the electrical conductivity, density, and kinematic viscosity of the fluid. We also use the Reynolds number

$$\mathrm{R} \equiv \frac{\delta_{\mathrm{Ha}} U}{\nu} = \frac{\mathrm{Re}}{\mathrm{Ha}} \tag{2}$$

based on the thickness of the Hartmann boundary layer $\delta_{\mathrm{Ha}} = a\mathrm{Ha}^{-1}$ as the length scale.

The results of the pioneering experiments [3] are of remarkably high quality and still have scientific value today. The experimental settings were pipes and ducts of different aspect ratios subjected to a uniform transverse magnetic field. The flows had moderate values of the Reynolds and Hartmann numbers. Laminarization was detected by comparing the measured pressure drop with theoretical values based on laminar MHD channel flow. The transition threshold could be associated with a certain value of R as a single controlling parameter.

Further experiments, a summary of which can be found in [5], extended the analysis to a wide range of Re and Ha as well, as in the case of a duct, various aspect ratios

$$\beta \equiv \frac{b}{a}. \tag{3}$$

Here b is the half-width in the direction perpendicular to the magnetic field. The special role of the parameter R was confirmed. It was found that at $\beta \geq 1$, both transition to turbulence and laminarization occurred near the threshold R_{cr} around 200, weakly depending on β. For β significantly smaller than unity, the experimental data were characterized by stronger scatter and showed R_{cr} decreasing with β as

$$\mathrm{R}_{\mathrm{cr}} \approx 215 - 85\exp(-0.35\beta). \tag{4}$$

The experimental results found confirmation in direct numerical (DNS) and large-eddy (LES) simulations conducted for duct and pipe flows at moderate Re and Ha, as in [6–9]. There, however, controversies and unanswered questions still remained. Particularly troubling was the disagreement with the results of linear stability analysis, which predicted R_{cr} two orders of magnitude higher than in the experiments [10]. Questions were also raised by high-Ha experiments [11, 12] that showed transition at $\mathrm{R}_{\mathrm{cr}} \approx 400$ in clear disagreement with $\mathrm{R}_{\mathrm{cr}} \approx 200$ found in earlier experiments at lower Ha.

A resolution of the controversies, which was both theoretically plausible and demonstrating a good quantitative agreement with the experiments, emerged in the recent computational works by the authors of this paper [1, 2, 13–18]. The starting point was the realization that the MHD flows in tubes belong to the class of wall-parallel flows, also including the hydrodynamic channel, pipe, duct, and plane Couette flows, for which the transition to turbulence cannot be explained by the linear instability mechanism. The transition requires a nonlinear interaction of perturbations growing to finite amplitudes. A likely scenario, which has been found to generate transition in good agreement with the experimental data, includes a transient algebraic growth of certain perturbations, whose amplitude increases by several orders of magnitude, and which experience secondary three-dimensional instabilities leading to turbulence.

As for the hydrodynamic flows in this class, the transition and laminarization in MHD tube flows do not have sharp thresholds, but rather occur in a range of R depending on the amplitude of added perturbations, wall roughness, inlet conditions, and other such factors. Furthermore, the behavior of transitional flow regimes, already intricate in the hydrodynamic case, is more complex in the MHD flow due to the particular boundary layer structure of the basic flow in the presence of a magnetic field. The computations [1, 2, 16, 18] have shown that at R approximately between 200 and 400, sustained turbulence exists near the sidewalls parallel to the imposed magnetic field. The core and Hartmann boundary layers of the flow remain laminar. The Hartmann layers become turbulent at $\mathrm{R} \approx 400$.

Appearance of turbulence localized near the side walls has not been detected in prior experimental studies conducted at high Ha. So far the only reliable experimental measurement in opaque liquid metal was the flow resistance coefficient, which, in such flows, is almost entirely dominated by the resistance in the Hartmann layers. This explains the fact that only the second transition in the Hartmann layers is often detected in high-Ha experiments as, e.g., in [12]. Progress in local velocity measurement in liquid metals may eventually provide a means for detecting turbulence at the side walls in experiments, e.g., by potential probes or by ultrasound Doppler velocimetry [19, 20]. We also remark that measurements in transitional flows face additional difficulties due to their high sensitivity to perturbations. For this reason, any interference by the measurement device should be avoided. Even in recent studies on the hydrodynamic pipe flow transition the total friction was used as the main diagnostic quantity since it can be determined with a minimum of interference [21].

The entire complex of questions of the transition and laminarization of MHD tube flows is discussed in detail in the recent review [22]. In this paper, we focus on a single aspect, namely, on the phenomenon of *patterned turbulence* – co-existence of intermittent laminar and turbulent zones, which, as we have shown in [1, 2], often characterizes the transitional flow regimes. Such flows are known to exist in hydrodynamic wall-bounded shear flows, e.g., as puffs and slugs in pipe flow [23]. Our work [1, 2] continued here is the first one, where patterned turbulence has been found in the MHD tubes. In this paper, we give a brief description of the phenomenon based on the earlier results and present new results concerning flows at high Hartmann numbers and the effect of the aspect ratio β.

1. Mathematical model and numerical method. We consider flows of incompressible, Newtonian, electrically conducting fluids (e.g., liquid metals) in a rectangular duct. The flow is subjected to a uniform magnetic field $\mathbf{B}$ perpendicular to the axis of the duct and parallel to one set of walls. Based on the assumption of small magnetic Reynolds and Prandtl numbers, the flows are described by the quasi-static approximation of the induction equation [24]. The governing equations and boundary conditions, non-dimensionalized using B, half-width a, mean velocity U, a/U, ρU^2, σUB, and UBa as respective scales, are

$$\begin{aligned}
\frac{\partial \mathbf{v}}{\partial t} + (\mathbf{v}\cdot\nabla)\mathbf{v} &= -\nabla p + \frac{1}{\mathrm{Re}}\triangle\mathbf{v} + N(\mathbf{j}\times\mathbf{e}), && (5)\\
\nabla\cdot\mathbf{v} &= 0, && (6)\\
\mathbf{j} &= (-\nabla\phi + \mathbf{v}\times\mathbf{e}), && (7)\\
\triangle\phi &= \nabla\cdot(\mathbf{v}\times\mathbf{e}), && (8)\\
\mathbf{v} &= \frac{\partial\phi}{\partial\mathbf{n}} = 0 \quad \text{at walls}, && (9)
\end{aligned}$$

where $\mathbf{v}$, p, $\mathbf{j}$, and ϕ are, respectively, the velocity, pressure, electrical current density and electric potential, $\mathbf{e}$ is the unit vector in the direction of the magnetic field, $\mathrm{N} = \mathrm{Ha}^2/\mathrm{Re}$ is the magnetic interaction parameter, and Ha and Re are the Hartmann and Reynolds numbers defined in Eq. (1).

The problem is solved numerically using our in-house solver based on the finite-difference method described as scheme B in [25]. The spatial discretization is of the 2^{nd} order on a non-uniform structured grid formed along the lines of the Cartesian coordinate system. The time integration is of the second order, explicit, and uses a projection-correction procedure to satisfy incompressibility. The computational grid can be clustered in the wall-normal directions to provide adequate resolution of the boundary layers using the coordinate transformation (see [16, 25] for detailed discussions)

$$z = a\frac{\tanh(A\zeta)}{\tanh(A)} \ \text{ or } \ z = \omega\sin\left(\frac{\pi}{2}\zeta\right) + (1-\omega)\zeta, \qquad (10)$$

where z stands for a wall-normal coordinate, ζ is the transformed coordinate, in which the grid is uniform, the clustering parameter A is typically between 2 and 2.5, and the parameter $\omega = 0.96$.

The computations were conducted as direct numerical simulations (DNS) for three-dimensional unsteady flows without any *a priori* assumptions about the flow dimensionality, symmetry, and spatial nature. As described in [1, 2, 16–18, 25], special care is taken to conduct simulations in sufficiently long domains and with sufficiently fine grids, so that the flow behavior at both large and small scales is accurately reproduced.

2. Patterned turbulence in ducts of square cross-section and in pipes at moderate Re **and** Ha**.** The simulations have been conducted for two settings: flows periodic in the streamwise direction and flows with non-periodic inlet/exit conditions. Periodic conditions represent a fully developed flow under a perfectly uniform magnetic field. The non-periodic formulation is more realistic and allows us to apply non-uniform magnetic fields with sharp gradients at the entry and exit of the test sections. By that it is possible to mimic the real flow conditions in experiments, where the magnetic field is never perfectly uniform and the flow evolution is influenced by entry effects.

The simulations are described in detail in [1, 2] and discussed in the general context of the transition in MHD tube flows in [22]. Here, we provide a brief summary necessary for understanding the new results.

We start with the results of periodic DNS [1], where flows in a pipe and in a duct of square cross-section are analyzed at moderate (3000 to 5000) values of Re.The key feature of these simulations is the large length of the computational domain, up to 64 π in terms of the hydraulic radius. As a result, previously unknown patterned turbulence regimes were observed for both the pipe and the duct. The regimes were realized in all DNS conducted within a certain range of Ha (e.g., at $\mathrm{Re} = 5000$, the range was $21 < \mathrm{Ha} < 26$ for the duct and $18 < \mathrm{Ha} < 23$ for the pipe). Below and above this range, all the simulations yielded, correspondingly, fully turbulent and fully laminar flows.

Two types of patterned turbulence regimes were found in [1]. In both, the flow has isolated turbulent spots near the sidewalls and is otherwise laminar. One type is the 'extended turbulent zone' observed in some simulations at low Ha close to the range of fully turbulent flow. The turbulent zone grows with time along the streamwise direction and eventually fills the entire length of the flow domain. The other type is a flow with turbulent 'puffs' – localized turbulent spots, which tend to exist for a very long time without strong changes in their kinetic energy and length. The latter is typically about 30 hydraulic radii. The puffs tend to form staggered patterns, although the specific arrangement is largely influenced by initial conditions. We have also analyzed the temporal evolution of the puffs and identified multiple events as, e.g., merging and splitting of two or more neighboring puffs, and two opposite-side spots forming a 'locked' state and travelling together.

In [2], we have extended the analysis to reproduce the real experimental conditions of the Hartmann and Lazarus setup [3] using transition simulations with in- and outflow conditions. They were performed at $\mathrm{Re} = 3000$. Turbulent conditions at the inlet were obtained from a periodic flow simulation running at the same Re and grid spacing. The streamwise domain size was chosen as $L_x = 128\pi$ to minimize the effects of the exit boundary conditions and provide more room for the spatial evolutionof turbulent spots. The results of these runs have confirmed the general conclusions from the simulations with periodic boundary conditions [1]. There exists a range of Ha ($12 \leq \mathrm{Ha} \leq 14$ in a square duct at $\mathrm{Re} = 3000$), in which the flow is neither fully laminar nor fully turbulent, but has isolated turbulent spots in the sidewall layers. The typical characteristics of these spots are similar to those found in [1]. Also, as demonstrated in [2], there is a remarkably good quantitative agreement between the non-dimensional pressure drop measured by Hartmann and Lazarus and computed in both periodic and non-periodic simulations.

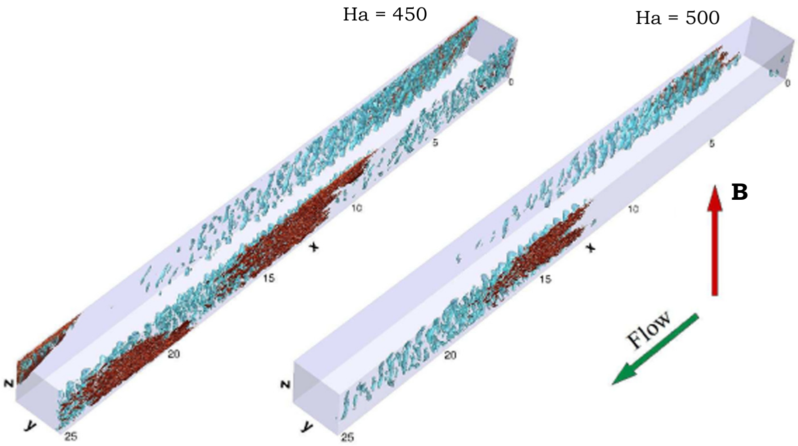

Fig. 1. Patterned turbulence regimes in duct flow at Re $= 10^5$ and Ha $=450$, 500. The isosurfaces of TKE (brown) of transverse velocity components corresponding to 2% of the maximum are shown, also shown are the isosurfaces of the second eigenvalue λ_2 (cyan) of the tensor $S_{ik}S_{kj} + \Omega_{ik}\Omega_{kj}$, where S and Ω are the rate of strain and vorticity tensors.

3. Patterned turbulence in the MHD duct at high Re **and** Ha**.** The DNS study of the MHD flow in a square duct at Re $= 10^5$ [16] with streamwise periodicity produced results largely consistent with the picture of laminar–turbulent transition obtained from the computations and experiments at moderate Re. In particular, we found the range $200 \leq$ Ha ≤ 350, i.e. $280 \leq R \leq 500$, between the fully laminar and fully turbulent states, where turbulence was sustained near the sidewalls, but the Hartmann layers and the core of the flow remained laminar. Patterned turbulence, however, was not found in [16], presumably because of the insufficient length $L_x = 4\pi$.

To address this issue, we conducted simulations at $L_x = 8\pi$. Each simulation lasted not less than 200 convective time units. The computational grid of $N_x \times N_y \times N_z = 2048 \times 385 \times 385$ points was used which was coarser than in [16], but, according to [16], sufficient for a qualitatively correct solution, whereas quantitative error in reproducing integral characteristics of the flow was within $2 \ldots 3\%$.

The results are illustrated in Fig. 1 for Ha $=450$ and 500 that corresponds to the transitional range of R $=$ Re/Ha ≈ 200. The flow is laminar in the core and in the Hartmann boundary layers, but has pronounced turbulent spots near the sidewalls. At Ha $=450$ (R $=222$, left-hand side plot) the flow is qualitatively similar to the flows with turbulent puffs found in simulations at moderate Re and Ha [1, 2]. We see sustained isolated turbulent spots, which maintain an approximately constant kinetic energy and length during the entire duration of the simulation. Furthermore, the typical length of a puff agrees between the moderate-Re and high-Re cases. In order to see that, we have to calculate the length in terms of the thickness of the sidewall (Shercliff) layer $\delta_{\mathrm{Sh}} \sim \mathrm{Ha}^{-1/2}$. The puffs at Ha $=450$ in Fig. 1 have $L_{\mathrm{puff}}/\delta_{\mathrm{Sh}} \approx 130 - 150$. For comparison, the puffs found in [1] for Re $=5000$ have $L_{\mathrm{puff}}/\delta_{\mathrm{Sh}} \approx 125 - 150$.

The right-hand side of Fig. 1 shows the results obtained at Re $= 10^5$ and Ha $=500$. In this case, all but one of attempts resulted in purely laminar states. One simulation, however, starting with an initial state at Ha $=450$ produced a flow with sustained turbulent spots. The spots are qualitatively similar to the puffs at Ha $=450$, but have a substantially lower turbulent kinetic energy and length $L_{\mathrm{puff}} \approx 85\delta_{\mathrm{Sh}}$.

We also notice that the appearance of isolated puffs is accompanied by quasi-$2D$ columnar vortices (cyan shading in Fig. 1), which were identified in our prior study [16] in the same range of Re and Ha. It appears that there is an interaction between the puffs and quasi-2D vortices, such that the puffs are seemingly stretched along the magnetic field direction. As a result, the turbulent spots exhibit a tendency to occupy the entire height of the sidewall layer and, thus, resemble objects known as "turbulent bands".

4. Effect of the aspect ratio of a duct. In order to explore the effect of the aspect ratio β on transitional flow regimes, we conducted additional DNS in a domain with streamwise periodicity. A domain of dimensions $L_x \times L_y \times L_z = 50 \times 8 \times 2$ with a grid of parameters $N_x \times N_y \times N_z = 1024 \times 512 \times 128$, $A_y = 2.3$, $A_z = 2.3$ (grid clustering coefficients in the y- and z-directions) was used. The magnetic field was in the z- or y-direction, which corresponded to $\beta = 4$ or $\beta = 1/4$. These configurations approach, respectively, the Hartmann channel flow and the channel flow with a spanwise magnetic field. Flows at $\mathrm{Re} = 5000$ were computed, which allowed us to directly compare with the results of [1] for $\beta = 1$. In order to minimize the effect of the stochastic nature of the transitional flow regimes, many simulations were repeated several times with various initial conditions.

The simulations have shown that the aspect ratio does not fundamentally change the nature of the transition. At $\beta = 1/4$ and 4, as in our earlier simulations [1, 2] at $\beta = 1$, we observed two threshold Hartmann numbers $\mathrm{Ha}_1 < \mathrm{Ha}_2$ such that the flow is consistently found purely laminar at $\mathrm{Ha} > \mathrm{Ha}_2$, fully turbulent at $\mathrm{Ha} < \mathrm{Ha}_1$ and demonstrating patterned turbulence with isolated turbulent spots in the sidewall layers and laminar Hartmann layers and in the core flow at $\mathrm{Ha}_1 \leq \mathrm{Ha} \leq \mathrm{Ha}_2$. Within this general scenario, however, some interesting new features have been found.

The typical structure of the flows with patterned turbulence is illustrated in Figs. 2 and 3. Visual and quantitative inspection of the isolated turbulent spots at $\beta = 4$ (see Fig. 2) shows no significant difference to the square duct case. The characteristics of the spots, such as the turbulent kinetic energy in transverse velocity components and the typical length are similar to those at $\beta = 1$. This allows us to identify them as turbulent puffs found earlier in [1, 2]. The only ascertainable novelty of the $\beta = 4$ case is that the sidewall layers and, thus, the turbulent spots are now separated by a much wider laminar core flow. This leads

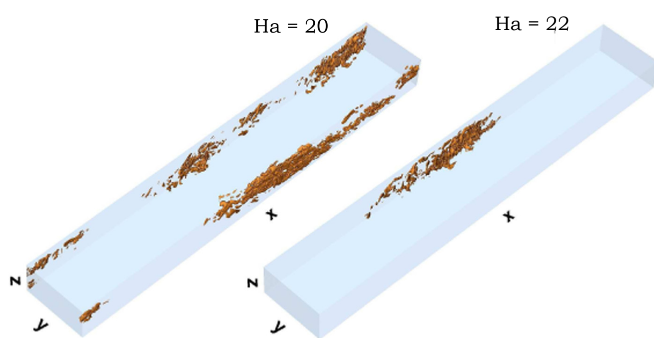

Fig. 2. Patterned turbulence regimes in a duct with $\mathrm{Re} = 5000$ and $\beta = 4$. The isosurfaces of turbulent kinetic energy of the transverse velocity components $u_y^2 + u_z^2$ are shown in the 3D domain for flows with $\mathrm{Ha} = 20$ and 22; the magnetic field is applied in the z-direction. The z-range is scaled by a factor of 2 to make the structures recognizable.

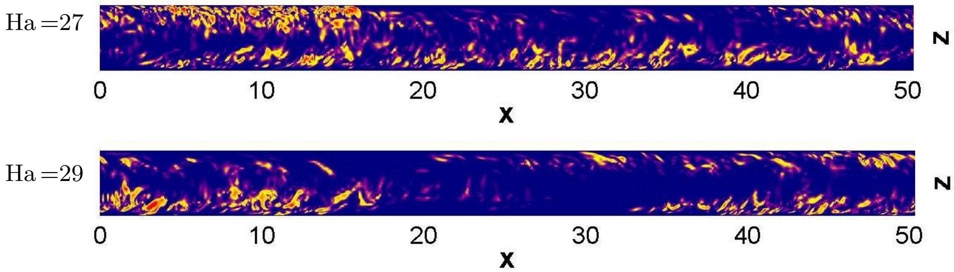

Fig. 3. Typical patterned turbulence structures in a duct with $\mathrm{Re} = 5000$ and $\beta = 1/4$. Instantaneous distributions of turbulent kinetic energy of the transverse velocity components $u_y^2 + u_z^2$ are shown in the (x, z)-cross-sections at $y = 0$ for flows with $\mathrm{Ha} = 27$ and 29. The magnetic field is applied in the y-direction, i.e. normal to the (x, z)-plane shown in the figure. The z-range is scaled by a factor of 2 to make the structures recognizable.

to loss of interaction between the spots forming at the opposite walls, which now appear to evolve as independent entities. In particular, as illustrated in Fig. 2, the spots do not form a staggered pattern – a tendency observed in [1, 2] for the square duct case.

Fig. 3 shows that the decrease of β to 1/4 means that each side layer occupies a larger fraction of the duct width b. As a result, the zone of the plug-like core flow separating the sidewall layers from each other is reduced or even disappears completely. This implies that a turbulent spot in one sidewall layer may induce turbulence within another layer at the opposite wall.

Another novelty of the $\beta = 1/4$ case is that clearly isolated puffs are observed only at Ha approaching Ha_2, i.e. at the high-Ha end of the transitional range. At lower Ha, turbulent spots tend to expand and gradually fill the entire length of the computational domain (see, e.g., flow at $\mathrm{Ha} = 27$ in Fig. 3). The velocity field within such spots is dominated by streamwise streaks – elongated zones of high or low streamwise velocity shown in Fig. 4*a*,*b*. One can see an analogy with the streak-dominated structure of the boundary layers found in simulations of the channel under a spanwise magnetic field [26] – a case closely corresponding to the duct with $\beta \ll 1$. One can see this similarity in Fig. 4c,d that shows a detailed view of the coherent near-wall structures for a channel flow at $\mathrm{Re} = 6667$ and $\mathrm{Ha} = 30$ (c) and a duct flow at $\mathrm{Re} = 5000$ and $\mathrm{Ha} = 29$ (d). The latter is a close-up of the red frame in Fig. 4b. The fact that patterned turbulence was not detected in our prior study [26] can be attributed to the small spanwise and streamwise size of the computational domain $L_x \times L_y = 2\pi \times \pi$, which is obviously smaller than the size of turbulent/laminar patches seen in Fig. 4*a*,*b*.

This was corrected in [27], where patterned turbulence in the form of oblique turbulent bands was observed at several sets of parameters including $\mathrm{Re} = 4000$, $\mathrm{Ha} = 22.4$ in a much larger domain size. This observation is fully supported by our results. As we can see, the coherent structures in Fig. 4a,b are also organized as turbulent patches in the form of oblique bands. It would be interesting to explore the observed similarity and the oblique nature of these bands in a broader parameter range, in particular, their existence in ducts of very low aspect ratio β.

Summarizing the results for non-square ducts, we can conclude that the aspect ratio of the duct has a not very strong but clearly discernable effect on the thresholds Ha_1 and Ha_2. Specifically, our simulations indicate that the most likely values are $\mathrm{Ha}_1 \approx 19$, $\mathrm{Ha}_2 \approx 23$ at $\beta = 4$, $\mathrm{Ha}_1 \approx 21$, $\mathrm{Ha}_2 \approx 25$ at $\beta = 1$ (see [1]), and $\mathrm{Ha}_1 \approx 27$, $\mathrm{Ha}_2 \approx 29$ at $\beta = 1/4$. This corresponds to a shift of the transitional

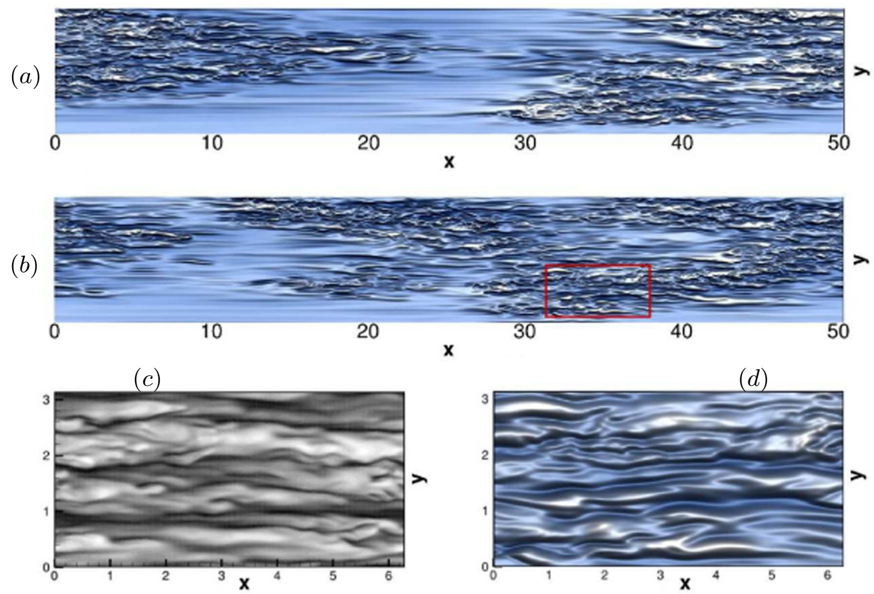

Fig. 4. Turbulent streaky patterns in the near-wall region for a duct flow with $\mathrm{Re} = 5000$ and $\beta = 1/4$ and a channel flow under a spanwise magnetic field. Instantaneous distributions of streamwise velocity fluctuations are shown for (*a*,*b*) duct flow at $\mathrm{Ha} = 29$ in the cross-sections $z = -0.9$ and $z = 0.9$ near the sidewalls and (*c*) channel flow at $\mathrm{Re} = 6667$ and $\mathrm{Ha} = 30$ in the section $z = 0.9$. Also shown is the close-up (*d*) into the duct flow indicated by the red frame in plot (*b*). Both plots (*c*) and (*d*) are of the same dimensions $2\pi \times \pi$, in all cases the magnetic field is applied in the y-direction.

range of Rr from $208 \leq \mathrm{R_{cr}} \leq 250$ at $\beta = 4$ to $200 \leq \mathrm{R_{cr}} \leq 238$ at $\beta = 1$ and to $172 \leq \mathrm{R_{cr}} \leq 185$ at $\beta = 1/4$. Such a behavior is consistent with the experimental observations collected in [5], where $\mathrm{R_{cr}}$ is found to decrease with decreasing β, in particular, with the empirical formula (4).

The change of $\mathrm{R_{cr}}$ with β is not an artifact of the stochastic nature of the transition. As already mentioned, we have minimized the influence of stochasticity by conducting multiple simulations of each case with various initial conditions. It is also not a numerical effect since the grid spacing was the same in all cases. Two possible qualitative explanations based on the flow physics can be suggested.

One explanation is geometrical. As already mentioned and illustrated in Figs. 2 and 3, the variation of β changes the width of the plug-like laminar flow zone separating the sidewall layers from large at $\beta = 4$ to zero at $\beta = 1/4$. Since the separation by a uniform velocity region is likely to limit the ability of turbulent spots at one wall to induce turbulence at the opposite wall, we conclude, in agreement with our computational results, that turbulence should be sustainable at higher Ha in flows with lower β.

Another plausible explanation can be found from the analysis of the laminar basic velocity profiles shown in Fig. 5. The relevant Reynolds number determining the transition within a sidewall layer should be based on the actual value of the plateau velocity U_{plat} in the core rather than on the mean flow velocity U, as it has been done so far in this paper. One can see in Fig. 5 that, for $\mathrm{Ha} = 25$, U_{plat} normalized by U differs significantly between the three different β. It is largest for the flow at $\beta = 1/4$ and smallest for the flow at $\beta = 4$. Correspondingly, if the transition occurs at approximately the same $\mathrm{R_{plat}} = U_{\mathrm{plat}}\delta_{\mathrm{Ha}}/\nu$ in all three cases, the

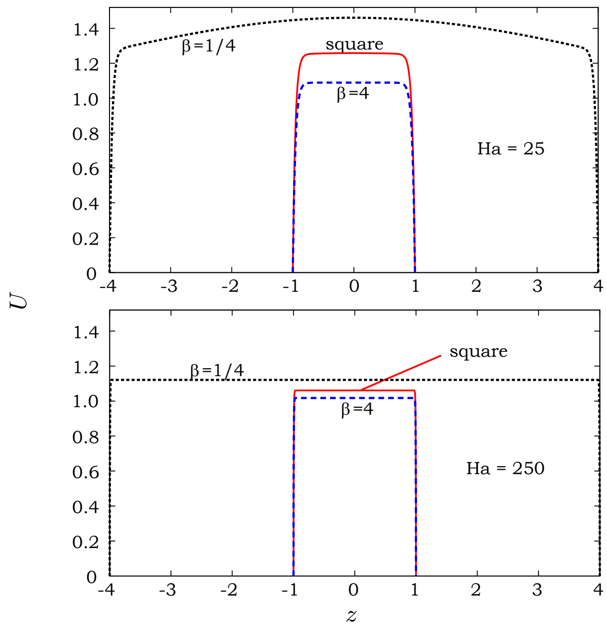

Fig. 5. Normalized velocity profiles of a laminar duct flow at $\mathrm{Ha} = 25$ and 250 showing Hartmann layers in the mid-plane cut at $y = 0$.

critical $\mathrm{R} = U\delta_{\mathrm{Ha}}/\nu$ must be the highest at $\beta = 4$ and lowest at $\beta = 1/4$. In fact, our data even support this explanation quantitatively. At $\mathrm{Ha} = 25$, the difference in maximum velocity and, hence, in local Reynolds number $\mathrm{R}_{\mathrm{plat}}$ amounts to $\pm 15\%$ with respect to the square duct. This leads almost exactly to the critical values of Ha_2 – for the case $\beta = 4$, the estimation yields $\mathrm{Ha}_2 = 25(\text{square}) \times 0.85 = 21.25$, and for $\beta = 1/4$, $\mathrm{Ha}_2 = 25(\text{square}) \times 1.15 = 28.75$. Both are very close to the critical values of Ha_2 identified in our simulations.

Neither of the two explanations would be valid in the case of high-Ha, high-Re flows. Firstly, the separation between the sidewall layers is always large unless extremely small values of β are considered. Secondly, as illustrated in Fig. 5 for $\mathrm{Ha} = 250$, the values of U_{plat} are only slightly affected by β – the relative difference in maximum velocity is about $\pm 3\%$. We should expect that β exerts only a weak influence on R_{cr}. This view is also suggested by our prior study of MHD duct flow at $\mathrm{Re} = 10^5$ and Ha up to 500 [16]. Here the results of DNS in a square duct have been compared with the experimental data of Murgatroyd [28] performed in a duct with $\beta = 5$ and the same range of Re and Ha. The comparison of the friction coefficient has shown that both experimental and numerical values practically collapse at $\mathrm{Ha} > 200$. Also, we identified that laminarization in both geometries occurred at the same critical $\mathrm{Ha}_2 \approx 500$.

5. Summary and conclusions. Our computational results confirm that the patterned turbulence is a robust feature of MHD tube flows. It has the form of a laminar state with isolated turbulent spots within the sidewall layers and appears in flows at high and low Reynolds numbers, in pipes and ducts of various aspect ratios.

The phenomenon of patterned turbulence deserves further consideration, especially in ducts with the low aspect ratio $\beta < 1$. It would be interesting in this regard to analyze transitional flow states in a channel with a spanwise magnetic field, where turbulent spots may be found in simulations in sufficiently long and wide computational domains.

Acknowledgements. TB and DK acknowledge financial support from the Helmholtz Alliance "Liquid Metal Technologies" and the Deutsche Forschungsgemeinschaft. OZ acknowledges financial support from the U.S. National Science Foundation (Grants CBET 0966557 and CBET 1232851). Computer resources were provided by the computing centers of Forschungszentrum Jülich (NIC) and TU Ilmenau.

REFERENCES

[1] D. Krasnov, *et al.* Patterned turbulence in liquid metal flow: Computational reconstruction of the Hartmann experiment. *Phys. Rev. Lett.*, vol. 110 (2013), p. 084501.

[2] O. Zikanov, *et al.* Patterned turbulence in spatially evolving magnetohydrodynamic tube flows. *Theor. Comp. Fluid Dyn.*, vol. 28 (2014), no. 3, pp. 319–334.

[3] J. Hartmann and F. Lazarus. Hg-dynamics II: Experimental investigations on the flow of mercury in a homogeneous magnetic field. *K. Dan. Vidensk. Selsk. Mat. Fys. Medd.*, vol. 15 (7) (1937), no. 7, pp. 1–45.

[4] J. Hartmann. Hg-dynamics I: Theory of the laminar flow of an electrically conductive liquid in a homogeneous magnetic field. *K. Dan. Vidensk. Selsk. Mat. Fys. Medd.*, vol. 15 (6) (1937), no. 6, pp. 1–28.

[5] H. Branover. *Magnetohydrodynamic Flow in Ducts* (Wiley, Hoboken NJ, New York, 1978).

[6] H. Kobayashi. Large eddy simulation of magnetohydrodynamic turbulent duct flows. *Phys. Fluids*, vol. 20 (2008), p. 015102.

[7] R. Chaudhary, S.P. Vanka, and B.G. Thomas. Direct numerical simulations of magnetic field effects on turbulent flow in a square duct. *Phys. Fluids*, vol. 22 (2010), no. 7, p. 075102.

[8] V. Shatrov and G. Gerbeth. Marginal turbulent magnetohydrodynamic flow in a square duct. *Phys. Fluids*, vol. 22 (2010), p. 084101.

[9] S. Satake, T. Kunugi, and S. Smolentsev. Direct numerical simulations of turbulent pipe flow in a transverse magnetic field. *J. Turb.*, vol. 3 (2002), pp. 27–29.

[10] R.J. Lingwood and T. Alboussière. On the stability of the Hartmann layer. *Phys. Fluids*, vol. 11 (1999), pp. 2058–2068.

[11] C.B. Reed and P.S. Lykoudis. The effect of a transverse magnetic field on shear turbulence. *J. Fluid Mech.*, vol. 89 (1978), pp. 147–171.

[12] P. Moresco and T. Alboussière. Experimental study of the instability of the Hartmann layer. *J. Fluid Mech.*, vol. 504 (2004), pp. 167–181.

[13] D.S. Krasnov, *et al.* Numerical study of instability and transition to turbulence in the Hartmann flow. *J. Fluid Mech.*, vol. 504 (2004), pp. 183–211.

[14] D. Krasnov, M. Rossi, O. Zikanov, and T. Boeck. Optimal growth and transition to turbulence in channel flow with spanwise magnetic field. *J. Fluid Mech.*, vol. 596 (2008), pp. 73–101.

[15] D. Krasnov, O. Zikanov, M. Rossi, and T. Boeck. Optimal linear growth in magnetohydrodynamic duct flow. *J. Fluid Mech.*, vol. 653 (2010), pp. 273–299.

[16] D.S. Krasnov, O. Zikanov, and T. Boeck. Numerical study of magnetohydrodynamic duct flow at high Reynolds and Hartmann numbers. *J. Fluid Mech.*, vol. 704 (2012), pp. 421–446.

[17] Y. Zhao, O. Zikanov, and D. Krasnov. Instability of magnetohydrodynamic flow in an annular channel at high Hartmann number. *Phys. Fluids*, vol. 23 (2011), p. 084103.

[18] Y. Zhao and O. Zikanov. Instabilities and turbulence in magnetohydrodynamic flow in a toroidal duct prior to transition in Hartmann layers. *J. Fluid Mech.*, vol. 692 (2012), pp. 288–316.

[19] C. Mistrangelo and L. Bühler. Perturbing effects of electric potential probes on MHD duct flows. *Exp. Fluids*, vol. 48 (2010), pp. 157–165.

[20] R. Nauber, *et al.* Novel ultrasound array measurement system for flow mapping of complex liquid metal flows. *Eur. Phys. J. Special Topics*, vol. 220 (2013), pp. 43–52.

[21] B. Hof, J. Westerweel, T.M. Schneider, and B. Eckhard. Finite lifetime of turbulence in shear flows. *Nature*, vol. 443 (2006), pp. 59–62.

[22] O. Zikanov, *et al.* Laminar-Turbulent Transition in Magnetohydrodynamic Duct, Pipe, and Channel Flows. *Appl. Mech. Rev.*, vol. 66 (2014), no. 3, p. 030802.

[23] I.J. Wygnanski and F.H. Champagne. On transition in a pipe. Part 1. The origin of puffs and slugs and the flow in a turbulent slug. *J. Fluid Mech.*, vol. 59 (1973), pp. 281–335.

[24] P.A. Davidson. *An Introduction to Magnetohydrodynamics* (Cambridge University Press, 2001).

[25] D. Krasnov, O. Zikanov, and T. Boeck. Comparative study of finite difference approaches to simulation of magnetohydrodynamic turbulence at low magnetic Reynolds number. *Comp. Fluids*, vol. 50 (2011), pp. 46–59.

[26] D. Krasnov, O. Zikanov, J. Schumacher, and T. Boeck. Magnetohydrodynamic turbulence in a channel with spanwise magnetic field. *Phys. Fluids*, vol. 20 (2008), no. 9, p. 095105.

[27] G. Brethouwer, Y. Duguet, and P. Schlatter. Turbulent-laminar coexistence in wall flows with Coriolis, buoyancy or Lorentz forces. *J. Fluid Mech.*, vol. 704 (2012), pp. 137–172.

[28] W. Murgatroyd. Experiments on magnetohydrodynamic channel flow. *Philos. Mag.*, vol. 44 (1953), pp. 1348–1354.

Received 15.01.2015